Absence of ferromagnetic-transport signatures in epitaxial paramagnetic and superparamagnetic $Zn_{0.95}Co_{0.05}O$ films

S. Ye,[1,4,*] V. Ney,[1] T. Kammermeier,[1] K. Ollefs,[1] S. Zhou,[2] H. Schmidt,[2] F. Wilhelm,[3] A. Rogalev,[3] and A. Ney[1]
[1]*Fachbereich Physik and Center for Nanointegration Duisburg-Essen (CeNIDE), Universität Duisburg-Essen, Lotharstrasse 1, D-47057 Duisburg, Germany*
[2]*Institut für Ionenstrahlphysik und Material forschung, Forschungszentrum Dresden–Rossendorf, D-01328 Dresden, Germany*
[3]*European Synchrotron Radiation Facility (ESRF), 6 Rue Jules Horowitz, BP 220, 38043 Grenoble Cedex, France*
[4]*Institute of Microelectronics and Information Technology, Wuhan University, Wuhan 430072, China*
(Received 24 June 2009; revised manuscript received 7 October 2009; published 23 December 2009)

Paramagnetic (PM) and superparamagnetic (SPM) $Zn_{0.95}Co_{0.05}O$ epitaxial films display similar temperature and magnetic field dependent anisotropic magnetoresistance (MR) effects. The high structural quality of the PM films is confirmed by x-ray linear dichroism. A classical two-band model describes these MR effects well and reveals the same intrinsic origin of the transport signatures in PM and SPM $Zn_{0.95}Co_{0.05}O$ films. The temperature-dependent resistivity of the respective films arises from a Mott variable-range hopping process. The absence of the anomalous Hall effect in the SPM film provides another evidence for lacking contributions from the SPM phase to the magnetotransport properties. Moreover, above the blocking temperature of SPM $Zn_{0.95}Co_{0.05}O$ films, the $M(H)$ curve can be described by a Langevin function, indicating the presence of approximately 2 nm large magnetic nanoparticles. Therefore, only the contribution of PM Co^{2+} ions in $Zn_{0.95}Co_{0.05}O$ films to the transport behavior can be found, thus demonstrating that 2 nm large magnetic Co nanoparticles does not interact with the carriers.

DOI: 10.1103/PhysRevB.80.245321 PACS number(s): 75.50.Pp, 75.70.Ak, 71.70.Ej, 72.20.Ee

I. INTRODUCTION

The search for possible spintronic materials aims at carrier-controlled ferromagnetism (FM) to realize multifunctional semiconductors. Mechanisms for FM order based on hole-mediated FM (Ref. 1) or the percolation of bound magnetic polarons[2] have been proposed and compared with experimental results predominantly for III(Mn)V dilute magnetic semiconductors (DMS),[3] indicating the decisive role of carriers in the existing FM DMS. On the other hand, the wide-band gap and the large exciton binding energy of ZnO,[4] together with the theoretical prediction[1] and early experimental observations of room-temperature FM,[5] have created lots of interest in $Zn_{1-x}Co_xO$ regarding its potential spintronic applications. However, the existence of room-temperature FM in $Zn_{1-x}Co_xO$ has remained a controversial subject over the recent years.[6–9] This controversy originates from the fact that it is experimentally very challenging to distinguish between magnetic contributions from phase coherent Co on Zn lattice sites and magnetic contributions from inhomogeneous Co/CoO nanoclusters, which are difficult to be detected even with high-resolution transmission electron microscopy (HRTEM),[10] and, in particular, random interstitial Co and amorphous secondary Co phases. Another important and yet not well-understood issue is the absence of a magnetic field induced metal-insulator transition and simultaneous giant negative magnetoresistance (MR) properties of intrinsic $Zn_{1-x}Co_xO$, which would be a typical signature of FM semiconductors. Moreover, only a few studies deal with the magnetotransport behavior due to the high resistance of $Zn_{1-x}Co_xO$ films,[11,12] when Co^{2+} ions are isovalently substituting for Zn^{2+} ions and where the occurrence of free charge carriers is only related with intrinsic donorlike defects. Therefore, more experimental effort is required to clarify the important relationship between the observed magnetic properties and their influence on the respective transport behavior.

In this paper, we demonstrate that high-quality $Zn_{0.95}Co_{0.05}O$ epitaxial films can be reproducibly fabricated by reactive magnetron sputtering. The proper incorporation of Co atoms on Zn lattice sites is verified by x-ray linear dichroism (XLD) measurements as done before.[6] Such samples are paramagnetic (PM) and can be tuned toward superparamagnetic (SPM) by decreasing the oxygen content in the sputter gas.[13] In the entire regime from PM to SPM, the temperature-dependent conductivity arises from thermally activated phonon-assisted variable hopping between impurity states. The conductivity and long-range SPM magnetic ordering are simultaneously increased as a result of annealing procedures and reduced oxygen content. However, no anomalous Hall effect is found in the SPM $Zn_{0.95}Co_{0.05}O$ films. Large positive MR effects which are described well by a two-band model, are observed for both PM and SPM $Zn_{0.95}Co_{0.05}O$ films at low temperatures, which are similar to those previously observed in other PM II(Mn)-VI DMS materials.[14] On the other hand, a strong anisotropic MR effect depending on the orientation of the magnetic field with respect to the c axis of $Zn_{1-x}Co_xO$ films is found for both types of films, consistent with the observed single-ion PM anisotropy in PM $Zn_{1-x}Co_xO$.[15] Therefore, the transport properties are independent on the observed inhomogeneous magnetic phase which causes the SPM in the transition regime. The SPM can be ascribed to ~ 2 nm Co nanoparticles, whose size is estimated from the blocking temperature and fitting a Langevin function to the $M(H)$ curves. The absence of additional FM transport signatures in the SPM $Zn_{0.95}Co_{0.05}O$ films highlights the lack of efficient coupling between developing secondary FM phases and the carrier system.

II. EXPERIMENTAL DETAILS

$Zn_{0.95}Co_{0.05}O$ films of typically 100 nm thickness were deposited on polished 10 mm × 10 mm × 0.5 mm *c*-plane single crystal Al_2O_3 (0001) sapphire substrates provided by Crystec GmbH. To avoid ferromagnetic contamination on the as-received substrates, a thorough cleaning procedure for all substrates with acetone, ethanol, and deionized water in an ultrasonic bath was performed for 10 min, each. The $Zn_{0.95}Co_{0.05}O$ films were grown in ultrahigh vacuum (UHV) by dc-reactive magnetron sputtering using a metallic ZnCo (5% Co) target. The sputtering rate was monitored by a quartz-crystal microbalance. The base pressure of the UHV system is $\leq 1 \times 10^{-9}$ mbar. The working pressure in the chamber during film deposition is 4×10^{-3} mbar. The ratio of Ar and O_2 flows are adjusted via separated mass flow controllers. Typically an Ar:O_2 ratio of 10:1 to 10:0.8 leads to structurally excellent PM $Zn_{0.95}Co_{0.05}O$ films whereas reducing the Ar:O_2 ratio to 10:0.5 turns the films to SPM with less perfect incorporation of Co on Zn substitutional sites.[13] The substrate temperature was kept at 350 °C during the preparation. The postgrowth annealing in ultrahigh vacuum was performed directly in the preparation chamber at 450 °C for 30 min.

The structure of the films was routinely investigated by x-ray diffraction (XRD) with a Philips PANalytical X'Pert PRO using Cu $K\alpha_1$ and $K\alpha_2$. A commercial superconducting quantum interference device (SQUID) magnetometer (Quantum Design magnetic property measurement System (MPMS) XL, 5 T) was used for the integral magnetic investigations. X-ray absorption near-edge spectra (XANES) and XLD measurements were taken at the ESRF ID12 beamline under 10° grazing incidence of the x-ray beam, using total fluorescence yield detection in backscattering geometry. A quarter wave plate was used to flip the linear polarization of the synchrotron light from vertical to horizontal for the XLD measurements.[16,17] X-ray magnetic circular dichroism (XMCD) measurements were taken with right and left circular polarized light in an external magnetic field of 6 T under 15° grazing incidence in total fluorescence yield with the synchrotron beam incident through a slotted Si photodiode. All XANES spectra were normalized with respect to the edge jump.

For transport measurements an Al/Ti bilayer is deposited as contact pads by shadow masking in order to obtain ohmic contacts. All electrical measurements have been carried out in the van-der-Pauw geometry. MR and Hall measurements were performed in a temperature range from 5 to 300 K and in external magnetic fields (H) up to 6 T. The proportionality between the measured voltage and the current was always checked to ensure ohmic behavior and the absence of self-heating. The magnetic field H was perpendicular or parallel to the sample plane for the anisotropic MR measurements. The standard procedure of reversing the direction of H was used to separate the resistance and Hall components of the voltage. The MR ratio is defined as $\Delta\rho(H)/\rho_0\% = [\rho(H) - \rho_0]/\rho_0 \times 100\%$, where ρ_0 and $\rho(H)$ are the resistivity in zero field and at an applied field H, respectively.

III. STRUCTURAL PROPERTIES

The $Zn_{0.95}Co_{0.05}O$ films were checked first by means of XRD $\omega-2\theta$ scans (not shown). Very clean wide-angle $\omega-2\theta$ spectra were obtained both for PM and SPM $Zn_{0.95}Co_{0.05}O$ films without any indication for secondary phases. The PM sample exhibits a full width at half maximum (FWHM) of 0.16° at the ZnO (002) reflection, indicating good long-range crystallographic order. The SPM $Zn_{0.95}Co_{0.05}O$ film has a FWHM of 0.39° showing a reduced structural quality. By the x-ray reflectivity measurements, it confirms the thickness of the PM and SPM samples for the XANES experiments is around 100 nm, respectively. Figure 1(a) presents two XANES spectra recorded with two orthogonal linear polarizations at the Co K edge of these two types of $Zn_{0.95}Co_{0.05}O$ films, and the respective XLD signals providing local structural information which is complementary to XRD. Spectral features as already reported for $Zn_{0.90}Co_{0.10}O$ films[6] such as a clear pre-edge feature at 7728 eV associated with the transition of Co 1s to the 4p-3d hybridized state in tetrahedral environment[18] are present in these $Zn_{0.95}Co_{0.05}O$ films. In addition, there is no obvious metallic Co or CoO contribution to the XANES spectra in the typical spectral range.[19] However, the peak at 7728 eV becomes less pronounced for the SPM film, indicating the onset of phase separation in this film with increasing metallicity. The XLD spectra of the PM $Zn_{0.95}Co_{0.05}O$ film show a maximum signal of $(32 \pm 1\%)$ at the Co K edge and of $(63 \pm 1\%)$ at the Zn K edge (not shown) with respect to the edge jump, convincingly indicating high local crystallographic ordering with about 90% Co^{2+} ions on substitutional Zn sites as derived by a direct comparison with earlier findings.[6] However, the XLD spectrum of the SPM sample only shows a maximum signal of $(26 \pm 1\%)$ at the Co K edge indicative of only ~75% substitutional Co^{2+}. Note that Co

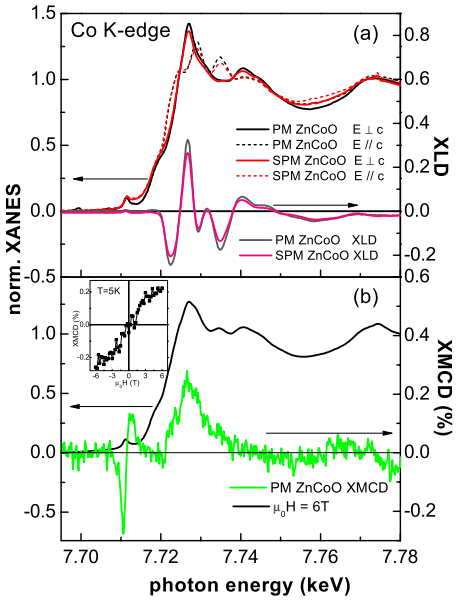

FIG. 1. (Color online) (a) XANES and XLD spectra of the paramagnetic $Zn_{0.95}Co_{0.05}O$ film (PM ZnCoO) and of the superparamagnetic $Zn_{0.95}Co_{0.05}O$ film (SPM ZnCoO) with the two orthogonal linear polarization directions at the Co K edge. (b) XMCD at the Co K edge recorded under 6 T at 5 K. The inset shows the magnetic field dependence of the XMCD at the pre-edge feature at 5 K for the PM ZnCoO.

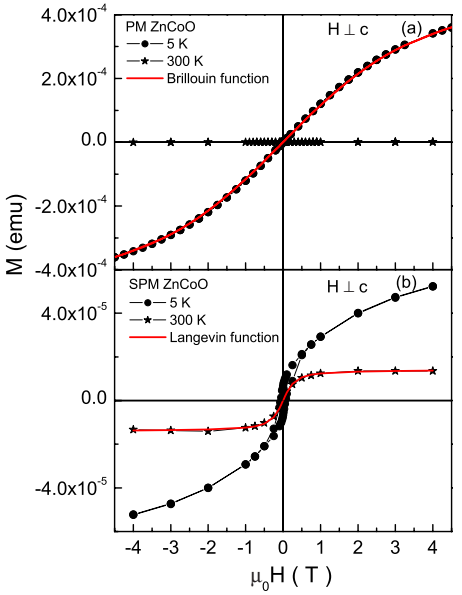

FIG. 2. (Color online) (a) $M(H)$ loops at 5 and 300 K with $H \perp c$ for the (a) PM ZnCoO and (b) SPM ZnCoO film.

on random interstitial sites or in a cubic environment would only reduce the amplitude of each feature of the XLD signal since they have no XLD signature. Therefore, the slightly reduced XLD signal observed in the SPM sample implies a remaining fraction of random interstitial Co atoms or Co/CoO suitable to account for magnetic clustering or phase separation, although hardly any difference in the XANES spectra compared to the PM sample is visible. Figure 1(b) displays the normalized Co K-edge XANES and the respective XMCD signal recorded under 6 T at 5 K for the PM $Zn_{0.95}Co_{0.05}O$ film. The clear dichroic signal at the pre-edge feature confirms the high probability of the Co^{2+} ions on substitutional Zn^{2+} sites. The magnetic field dependence of the XMCD at the pre-edge feature was recorded as well, presenting a Brillouin-type PM behavior, as shown in the inset of Fig. 1(b). Therefore, the XRD, XLD, and XMCD results demonstrate the high quality of the studied films with PM Co^{2+} ions on substitutional Zn sites. Importantly, different from other reports,[5] such high-quality $Zn_{0.95}Co_{0.05}O$ epitaxial films can be obtained reproducibly from one growth run to another (not shown). The XMCD spectrum of the SPM sample was measured as well and shows a slight reduction in the dichroic signal at the pre-edge feature and an increased negative dichroic signal between pre-edge feature and the main absorption edge (not shown), which is indicative of an increasing elemental character of the Co.[19]

IV. INTEGRAL MAGNETIC PROPERTIES

Figure 2 and the inset of Fig. 5 display the $M(H)$ loops and field-cooled/zero-field-cooled (FC/ZFC) $M(T)$ curves measured while warming from 5 to 300 K under an applied magnetic field of 100 Oe for these two kinds of $Zn_{0.95}Co_{0.05}O$ films, respectively. For the FC measurement, a large field of 40 kOe was applied during cooling down the sample from 300 to 5 K, whereas for the ZFC data the sample was cooled down without an applied magnetic field prior to the $M(T)$ measurement. For the sample with high structural quality, no hysteresis can be observed from 300 to 5 K, and the $M(H)$ curve at 5 K of this sample can be fitted well with a Brillouin function for $S=3/2$ and $L\sim 1$ as discussed in Ref. 6. The coinciding FC and ZFC curves in the entire measured temperature regime [inset of Fig. 5(a)] demonstrate the absence of FM. For $Zn_{0.95}Co_{0.05}O$ samples with reduced oxygen content in the sputter gas, a clear blocking behavior around 30 K is observed in the FC/ZFC curves. Consistently, the $M(H)$ curve exhibits a magnetic hysteresis at 5 K and a s-shaped anhysteretic $M(H)$ curve above the blocking temperature, indicative of SPM. Note that the data are not scaled to the sample volume so that the magnetization values of the PM and SPM sample cannot directly be compared. The $M(H)$ curve at 300 K of this sample can be described well by a Langevin function, $M/M_S(T=0) = \coth(\mu H/kT) - kT/\mu H$ with $\mu \approx 3600\mu_B$ being the particle's supermoment. The particle size can be inferred from this Langevin fit using a magnetic moment of Co of $1.75\mu_B$, which yields a mean diameter on the order of 2 nm. Furthermore, from the blocking temperature T_B and using $K_A V = 25k_B T_B$ for SPM nanoparticles,[20] where $K_A = 4.5 \times 10^6$ erg/cm^3 is the magnetic anisotropy of Co metal, V is the volume of the particle, k_B is the Boltzmann constant, and $T_B \sim 28$ K from Fig. 5 is the blocking temperature, the estimated particle mean diameter is ~ 2 nm. Therefore, the SQUID measurements provide evidence for an inhomogeneous SPM phase which is composed of phase-separated Co nanoclusters with a mean diameter of around 2 nm. These nanoclusters are hard to be detected by the conventional characterization techniques (such as XRD or HRTEM), especially when the Co is interstitial or in an amorphous phase. However, these results are in agreement with the reduced XLD signal of the SPM sample.

V. TRANSPORT MEASUREMENTS

By resistivity and Hall measurements, we find that the conductivity and carrier concentrations of the SPM films are two orders of magnitude larger than that for the PM films. Figure 3 shows the temperature dependence of the sheet resistance at zero magnetic field, which is found to be identical for both orientations (in-plane and out-of-plane geometry) of both PM and SPM samples, as expected thus ruling out background issues. Moreover, for better comparison, the temperature dependence of the sheet resistance at zero magnetic field of PM and SPM ZnCoO are normalized at R (300 K), as seen in the Fig. 3. The $R(T)$ dependence for both samples can be described by the Mott variable-range hopping (VRH) model, $\rho = A_0 \exp(T_0/T)^{1/4}$, indicating that the thermally activated phonon-assisted VRH between impurity states dominates the conductivity behavior, where A_0 and T_0 are fitting parameters.[21] T_0 is ~ 3000 and ~ 200 K for the PM and SPM sample, respectively. Our results of SPM $Zn_{0.95}Co_{0.05}O$ for T_0 is ~ 3000 K is consistent with that of Behan *et al.*,[22] where it was shown that strong FM only occurs when T_0 exceeds $>10\,000$ K. The electron concentration determined from the slope of the Hall measurements amounts to 2.4

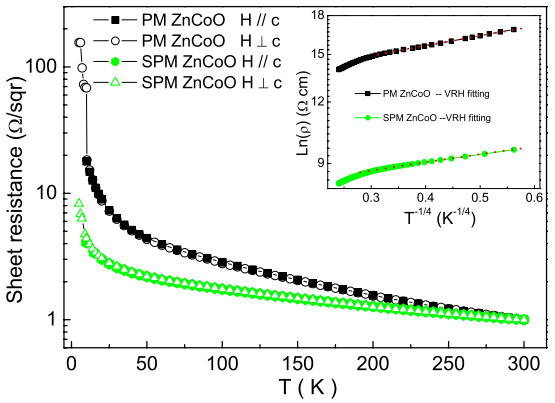

FIG. 3. (Color online) The temperature dependence of the sheet resistance ($H\|c$ and $H\perp c$) at zero magnetic field of both PM ZnCoO and SPM ZnCoO normalized at R (300 K). The inset shows the VRH fitting, respectively.

$\times 10^{17}$ and 2.5×10^{19} cm^{-3} for the PM and SPM samples, respectively. Considering the static magnetic polaron theory of Coey *et al.*,[2] increasingly mobile carriers should be inimical to magnetic order. Therefore, in the SPM $Zn_{0.95}Co_{0.05}O$ films, the transport behavior of carriers in the framework of the VRH theory is inconsistent with the magnetic properties in regard of the suggested mechanism for FM in $Zn_{1-x}Co_xO$ based on magnetic polarons.

Figures 4(a)–4(d) depicts the magnetic field dependence of the MR effect of the PM and SPM $Zn_{0.95}Co_{0.05}O$ films with the applied magnetic field parallel or perpendicular to the c axis, respectively. It can be found that the MR effect is independent on whether the $Zn_{0.95}Co_{0.05}O$ films are PM or SPM, and no open or "butterfly" MR (H) loop can be found in both samples. On the other hand, the MR effect has strong temperature dependence as shown in Fig. 5. Compared with the FC/ZFC $M(T)$ curves for PM and SPM samples in the insets of Fig. 5, the temperature dependence of the MR at 6 T exhibits a PM-like trend for both samples without any phenomenon corresponding to the blocking behavior. A large positive MR effect at 5 K is observed for both types of samples as shown in Fig. 4 and is similar to that known in PM II(Mn)-VI DMS compounds such as n-type conducting $Cd_{0.99}Mn_{0.01}Se$,[14] confirming the important contribution of the substituting 3d transition metals to the magnetotransport in the PM DMS. Therefore, for both of PM and SPM samples, they only display the MR transport behavior typical for PM. The positive MR decreases quickly with increasing temperature. At around 50 K, the positive MR changes to a negative MR effect similar to that observed in undoped ZnO,[23] which persists up to around 300 K. However, the curvature, the saturation, and the intensity of the obtained PM MR (H) effects at low temperatures are strongly dependent on the concentration of substituted Co^{2+} on Zn sites, and the orientation between the applied magnetic field and c axis of the films. The lower intensity of the positive MR in the SPM sample suggests a lower concentration of PM Co^{2+} ions on substitutional Zn sites, indicating that a fraction of Co can be located on random interstitial sites or as phase-separated Co nanoclusters, which is consistent with the observations by XLD. Moreover, as it can be found in Figs. 4(a) and 4(c),

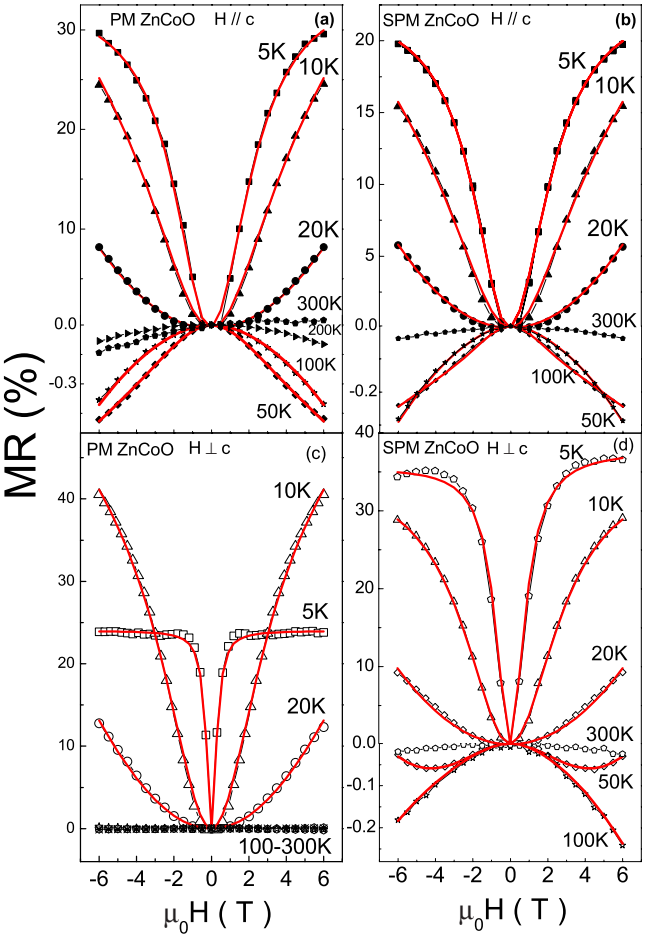

FIG. 4. (Color online) Measured and fitted (solid lines) magnetic field dependence of the MR effects for PM ZnCoO (a) $H\|c$ and (c) $H\perp c$ and for SPM ZnCoO (b) $H\|c$ and (d) $H\perp c$, in the temperature range from 5 to 300 K.

with the applied magnetic field changing from parallel to perpendicular to the c axis of PM $Zn_{0.95}Co_{0.05}O$ film, the large positive MR (H) at 5 K responds much faster to the

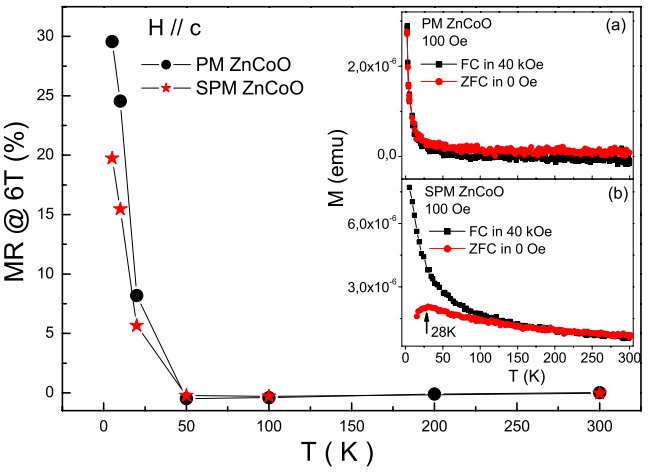

FIG. 5. (Color online) Temperature dependence of MR @ 6 T with $H\|c$ for two types of $Zn_{0.95}Co_{0.05}O$ films. The insets show the FC/ZFC $M(T)$ curves for (a) PM ZnCoO and (b) SPM ZnCoO.

TABLE I. Temperature-dependent distribution of the carrier concentration, conductivity, and mobility in two bands for SPM ZnCoO.

Two band parameters	5 K $H\|\|c$	10 K $H\|\|c$	20 K $H\|\|c$	5 K $H\perp c$	10 K $H\perp c$	20 K $H\perp c$
Band 1						
n_1 (10^{19} cm^{-3})	1.684	1.459	1.175	1.886	1.620	1.175
σ_1 (1/ohm cm)	2.795	5.977	9.943	0.118	3.810	9.900
β_1 (cm^2/V s)	1.036	2.557	5.282	0.039	1.468	5.258
Band 2						
n_2 (10^{19} cm^{-3})	0.266	0.891	1.175	0.064	0.730	1.175
σ_2 (1/ohm cm)	1.419	0.871	0.058	4.096	3.039	0.101
β_2 (cm^2/V s)	3.326	0.610	0.031	39.772	2.598	0.054

applied magnetic field and saturates at 1.2 T. Similar anisotropy of the MR effect is also observed in SPM $Zn_{0.95}Co_{0.05}O$ film as shown in Figs. 4(b) and 4(d) but the saturation field shifts to a higher value around 4 T due to the less substituted Co^{2+} on Zn sites. The enhanced positive MR with applied magnetic field perpendicular to the c axis is in agreement with the observed single-ion PM anisotropy,[15] indicating the coincidence between the PM magnetotransport and magnetization behavior in the PM $Zn_{1-x}Co_xO$ films. However, the saturation behavior at low magnetic field of the large positive MR effect has no corresponding saturated magnetization behavior shown on the $M(H)$ curve at 5 K with magnetic field perpendicular to the c axis of the film.

For the SPM sample with higher conductivity and carrier concentration $k_F\ell$ can be calculated and amount to ~ 0.06, i.e., $k_F\ell \ll 1$, using $k_F\ell = \hbar(3\pi^2)^{2/3}/(e^2\rho n^{1/3})$, where k_F is the Fermi wave vector, ℓ is the mean-free path, $\hbar$ is the Planck constant, e is the electron charge, ρ is the resistivity, and n is the electron concentration. Thus, the SPM sample is not in the weakly localized regime as described by Dietl *et al.*[24] On the other hand, one can assume the coexistence of two bands with different conductivities and mobilities due to the substituting PM Co^{2+} ions which have a narrow $3d$ band structure. The redistribution of carriers in the relative populations in these two bands is dominated by the temperature-dependent spin-splitting effect and thermally activated energy. Such a semiempirical two-band model[23,25] can fit the large positive MR effect at low temperature quite well as shown in Fig. 4. Calculations in the framework of such a model show that the MR can be given by $\Delta\rho(H)/\rho_\circ = aH^2/(b^2+cH^2)$, where $a = \sigma_1\sigma_2(\beta_1+\beta_2)^2$, $b=\sigma_1+\sigma_2$, and $c=(\beta_1\sigma_2-\beta_2\sigma_1)^2$, where the two-band conductivities σ_1, σ_2 and mobilities β_1, β_2, are fitting parameters. With increasing temperature, the MR obeys $\Delta\rho(H)/\rho_\circ \sim H^2 + aH^2/(b^2+cH^2)$ dependence, and the first term due to parabolic behavior dominates the MR effects at higher temperatures.

Table I lists the values of the fit parameters n_1, σ_1, β_1, n_2, σ_2, β_2 in two bands from 5 to 20 K for SPM ZnCoO with applied magnetic field parallel and perpendicular to the c axis, where $n=n_1+n_2$ and $\sigma=\sigma_1+\sigma_2$ are carrier concentration and conductivity extracted from experimental resistivity and Hall measurements, respectively. Note, that Hall measurements on PM samples could only be carried out at 300 K due to the extremely high resistivity PM samples, therefore we cannot provide the corresponding data for the PM sample. The largest positive MR has been observed at 5 K with the biggest difference between the carrier concentrations in these two bands. At $T=20$ K, with the same carrier concentration in the two bands, the MR effect shows a paraboliclike behavior, which can be understood by the $3d$ band moving away from the Fermi level with increasing temperature as reflected by the decreasing spin-splitting effect according to the decrease in the magnetization. The most interesting fitting result is the anisotropic mobility for band 2 at 20 K, where $\beta_\perp/\beta_\| = 1.74$, is in a good agreement with an early theoretical prediction[26] of $\beta_\perp/\beta_\| = 1.75$ in which the anisotropy of the wurtzite structure is taken into account for ZnO. This suggests that the less Co^{2+} ions and the decreasing spin-splitting effect by the increasing of the temperature lead to the properties of the $Zn_{1-x}Co_xO$ films are more closer to that in ZnO. With the temperature about 50 K, the negative MR also found in n-type conducting ZnO films dominates the transport properties. Moreover, with the applied magnetic fields switching from parallel to perpendicular to the c axis, the mobility decreases with increasing carrier concentration, indicating an enhanced localization of the carriers, which may lead to the increasing positive MR effect. The small mobility for both bands can be due to the grain boundaries in the ZnCoO films.[27] This classical two band model sheds light on the observed various positive or negative MR effects in $Zn_{1-x}Co_xO$ films prepared by different fabrication methods, which are dominated by the carrier concentration and mobility distribution of $3d$ states and impurities states at the Fermi level. Taking the above arguments into account, both the PM and SPM $Zn_{0.95}Co_{0.05}O$ films only present PM MR effects without any magnetic field driven long-range ordering of spin carrier transport, i.e., the absence of ferromagnetic electron transport. In addition, phase-separated Co nanoclusters do not influence the MR properties.

Hall measurements as depicted in Fig. 6 were carried out on the SPM sample in the same temperature and magnetic field range as the MR measurements. The Hall data show a perfectly linear behavior at 300 K in the whole measured magnetic field range as seen from the inset of Fig. 6. On the other hand, the weak temperature-dependent Hall effect as shown in Fig. 6 is inconsistent with the anomalous Hall effect caused by a spin-orbit coupling which is strongly temperature dependent. The Hall measurements at 5 K of the

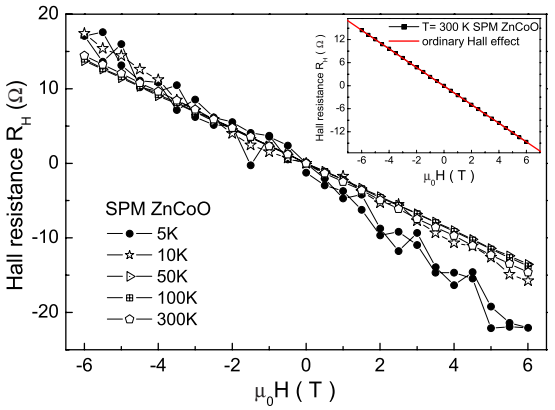

FIG. 6. (Color online) Hall resistance for SPM ZnCoO from 5 to 300 K. The inset is the ordinary Hall effect fitting for SPM ZnCoO at $T=300$ K.

highly resistive $Zn_{0.95}Co_{0.05}O$ films show an enhanced signal-to-noise ratio due to the detection limit of the setup. The small deviation from linearity at 5 K under high magnetic fields may be due to the redistribution of density of states by a local spin splitting of 3*d* states. This result demonstrates that also in SPM $Zn_{0.95}Co_{0.05}O$ films with the electron concentration amounting to 2.5×10^{19} cm^{-3}, i.e., around the critical electron concentration in ZnO,[11] no anomalous Hall effect is observed. Therefore, the PM and SPM $Zn_{0.95}Co_{0.05}O$ films reveal the same spin-scattering origin and the FM coupling mediated by the carriers responsible for the SPM may be excluded.

VI. CONCLUSION

$Zn_{0.95}Co_{0.05}O$ epitaxial films can be obtained with reproducible quality by UHV-magnetron reactive sputtering. The high local structural quality is confirmed by means of XRD and XLD measurements. Both conductivity and integral magnetic properties can be modified by reducing the oxygen content in the sputter gas. In contrast to the magnetotransport properties, the magnetic properties probed by SQUID reveal distinct differences ranging from paramagnetism to superparamagnetism. Randomly substituted Co^{2+} ions cause the similar positive MR effect described by a classical two-band model, both for the PM and SPM $Zn_{0.95}Co_{0.05}O$ films, which has been found in the PM II(Mn)-VI DMS as well. The absence of the anomalous Hall effect and the inconsistence of the VRH parameter T_0 with magnetic order described by the bound magnetic polaron theory prove the lack of FM electron transport signatures in the SPM $Zn_{0.95}Co_{0.05}O$ films. The smaller positive MR effect observed in the SPM $Zn_{0.95}Co_{0.05}O$ film compared to the PM $Zn_{0.95}Co_{0.05}O$ film with the same Co content, hints toward less substituted Co^{2+} ions in the SPM sample. XLD and $M(H)$ curves results demonstrate a remaining fraction of random Co being not located on substitutional Zn lattice sites. An inhomogeneous SPM phase which is constituted by phase-separated Co nanoclusters with a diameter of ~2 nm revealed by SQUID is found in the SPM $Zn_{0.95}Co_{0.05}O$ films. However, this SPM ensemble has no significant influence on the magnetotransport properties, revealing the same intrinsic origin of the observed transport behavior independent on the variation in the magnetization in PM and SPM $Zn_{0.95}Co_{0.05}O$ films.

ACKNOWLEDGMENTS

This work was supported by the European Union under the Marie-Curie Excellence Grant No. MEXT-CT-2004-014195, of the Sixth Framework Programme, and by the BMBF (Grant No. FKZ 03N8708).

*shuangli.ye@uni-due.de

[1] T. Dietl, H. Ohno, F. Matsukura, J. Cibert, and D. Ferrand, Science **287**, 1019 (2000).
[2] J. M. D. Coey, M. Venkatesan, and C. B. Fitzgerald, Nature Mater. **4**, 173 (2005).
[3] T. Dietl, H. Ohno, and F. Matsukura, Phys. Rev. B **63**, 195205 (2001).
[4] D. C. Look, Mater. Sci. Eng., B **80**, 383 (2001).
[5] K. Ueda, H. Tabata, and T. Kawai, Appl. Phys. Lett. **79**, 988 (2001).
[6] A. Ney, K. Ollefs, S. Ye, T. Kammermeier, V. Ney, T. C. Kaspar, S. A. Chambers, F. Wilhelm, and A. Rogalev, Phys. Rev. Lett. **100**, 157201 (2008).
[7] J. R. Neal, A. J. Behan, R. M. Ibrahim, H. J. Blythe, M. Ziese, A. M. Fox, and G. A. Gehring, Phys. Rev. Lett. **96**, 197208 (2006).
[8] K. R. Kittilstved, N. S. Norberg, and D. R. Gamelin, Phys. Rev. Lett. **94**, 147209 (2005).
[9] S. Zhou, K. Potzger, J. von Borany, R. Grötzschel, W. Skorupa, M. Helm, and J. Fassbender, Phys. Rev. B **77**, 035209 (2008).
[10] M. Opel, K.-W. Nielsen, S. Bauer, S. T. B. Goennenwein, J. C. Cezar, D. Schmeisser, J. Simon, W. Mader, and R. Gross, Eur. Phys. J. B **63**, 437 (2008).
[11] Q. Xu, L. Hartmann, H. Schmidt, H. Hochmuth, M. Lorenz, R. Schmidt-Grund, C. Sturm, D. Spemann, and M. Grundmann, Phys. Rev. B **73**, 205342 (2006).
[12] Q. Xu, L. Hartmann, H. Schmidt, H. Hochmuth, M. Lorenz, D. Spemann, and M. Grundmann, Phys. Rev. B **76**, 134417 (2007).
[13] S. Ye, V. Ney, T. Kammermeier, K. Ollefs, A. Ney, F. Wilhelm, and A. Rogalev, J. Supercond. Novel Magn. (to be published 2009).
[14] M. Sawicki, T. Dietl, J. Kossut, J. Igalson, T. Wojtowicz, and W. Plesiewicz, Phys. Rev. Lett. **56**, 508 (1986).
[15] P. Sati, R. Hayn, R. Kuzian, S. Régnier, S. Schäfer, A. Stepanov, C. Morhain, C. Deparis, M. Laügt, M. Goiran, and Z. Golacki, Phys. Rev. Lett. **96**, 017203 (2006).
[16] E. Sarigiannidou, F. Wilhelm, E. Monroy, R. M. Galera, E. Bellet-Amalric, A. Rogalev, J. Goulon, J. Cibert, and H. Mariette, Phys. Rev. B **74**, 041306(R) (2006).
[17] A. Rogalev, J. Goulon, C. Goulon-Ginet, and C. Malgrange, Lect. Notes Phys. **565**, 61 (2001).

[18] A. Barla, G. Schmerber, E. Beaurepaire, A. Dinia, H. Bieber, S. Colis, F. Scheurer, J.-P. Kappler, P. Imperia, F. Nolting, F. Wilhelm, A. Rogalev, D. Müller, and J. J. Grob, Phys. Rev. B **76**, 125201 (2007).

[19] K. Rode, R. Mattana, A. Anane, V. Cros, E. Jacquet, J.-P. Contour, F. Petroff, A. Fert, M.-A. Arrio, Ph. Sainctavit, P. Bencok, F. Wilhelm, N. B. Brookes, and A. Rogalev, Appl. Phys. Lett. **92**, 012509 (2008).

[20] J. L. Dormann, D. Fiorani, and E. Tronc, J. Magn. Magn. Mater. **202**, 251 (1999).

[21] N. F. Mott, Philos. Mag. **19**, 835 (1969).

[22] A. J. Behan, A. Mokhtari, H. J. Blythe, D. Score, X.-H. Xu, J. R. Neal, A. M. Fox, and G. A. Gehring, Phys. Rev. Lett. **100**, 047206 (2008).

[23] F. Reuss, S. Frank, C. Kirchner, R. Kling, Th. Gruber, and A. Waag, Appl. Phys. Lett. **87**, 112104 (2005).

[24] T. Dietl, T. Andrearczyk, A. Lipinska, M. Kiecana, M. Tay, and Y. Wu, Phys. Rev. B **76**, 155312 (2007).

[25] E. Zaremba, Phys. Rev. B **45**, 14143 (1992).

[26] E. Ziegler, A. Heinrich, H. Oppermann, and G. Stöver, Phys. Status Solidi A **66**, 635 (1981).

[27] A. H. Jayatissa, Semicond. Sci. Technol. **18**, L27 (2003).